

Discovery of 2-[3,5-Dichloro-4-(5-isopropyl-6-oxo-1,6-dihydropyridazin-3-yloxy)phenyl]-3,5-dioxo-2,3,4,5-tetrahydro[1,2,4]triazine-6-carbonitrile (MGL-3196), a Highly Selective Thyroid Hormone Receptor β Agonist in Clinical Trials for the Treatment of Dyslipidemia

Martha J. Kelly,^{*,†} Sherrie Pietranico-Cole,[‡] J. Douglas Larigan,[‡] Nancy-Ellen Haynes,[‡] Charles H. Reynolds,[§] Nathan Scott,[‡] John Vermeulen,[‡] Mark Dvorozniak,[‡] Karin Conde-Knape,[‡] Kuo-Sen Huang,[‡] Sung-Sau So,[‡] Kshitij Thakkar,[‡] Yimin Qian,[‡] Bruce Banner,[‡] Frank Mennona,[‡] Sara Danzi,^{||} Irwin Klein,[⊥] Rebecca Taub,[†] and Jefferson Tilley[‡]

[†]Madrigal Pharmaceuticals, Inc., Fort Washington, Pennsylvania 19034, United States

[‡]Hoffmann-La Roche, Inc., Nutley, New Jersey 07110, United States

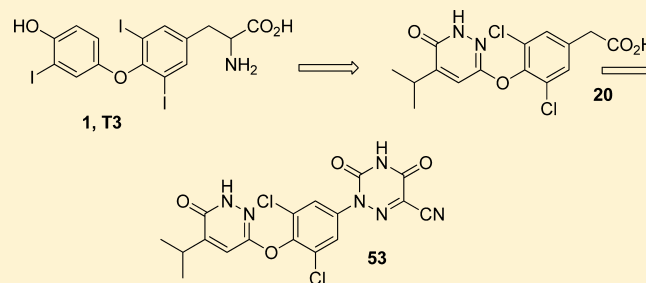
[§]Gfree Bio LLC, Doylestown, Pennsylvania 18902, United States

^{||}Queensborough Community College, Bayside, New York 11364, United States

[⊥]New York University School of Medicine, New York, New York 10016, United States

S Supporting Information

ABSTRACT: The beneficial effects of thyroid hormone (TH) on lipid levels are primarily due to its action at the thyroid hormone receptor β (THR- β) in the liver, while adverse effects, including cardiac effects, are mediated by thyroid hormone receptor α (THR- α). A pyridazinone series has been identified that is significantly more THR- β selective than earlier analogues. Optimization of this series by the addition of a cyanoazauracil substituent improved both the potency and selectivity and led to MGL-3196 (**53**), which is 28-fold selective for THR- β over THR- α in a functional assay. Compound **53** showed outstanding safety in a rat heart model and was efficacious in a preclinical model at doses that showed no impact on the central thyroid axis. In reported studies in healthy volunteers, **53** exhibited an excellent safety profile and decreased LDL cholesterol (LDL-C) and triglycerides (TG) at once daily oral doses of 50 mg or higher given for 2 weeks.



INTRODUCTION

Despite the success of statins in lowering LDL cholesterol (LDL-C) and thereby reducing cardiovascular disease, there is a need for new drugs for the treatment of dyslipidemia. Up to 10% of hypercholesterolemic patients do not tolerate statins, and roughly 70% of high risk cardiovascular patients do not achieve LDL-C goals.^{1,2} Diabetes is characterized by a particular form of dyslipidemia including elevated triglycerides (TG), low HDL cholesterol (HDL-C), and nonalcoholic fatty liver disease (NAFLD), and 60–75% of diabetics die of macrovascular cardiovascular disease.³ Drugs that lower fatty acid accumulation and degeneration in the liver may also be useful in the treatment of nonalcoholic steatohepatitis (NASH).⁴

The beneficial metabolic effects on cholesterol and TG levels of triiodothyronine (T3) **1** and its prohormone thyroxine (T4) have been known for many years. In part because of associated hypercholesterolemia, hypothyroidism is associated with

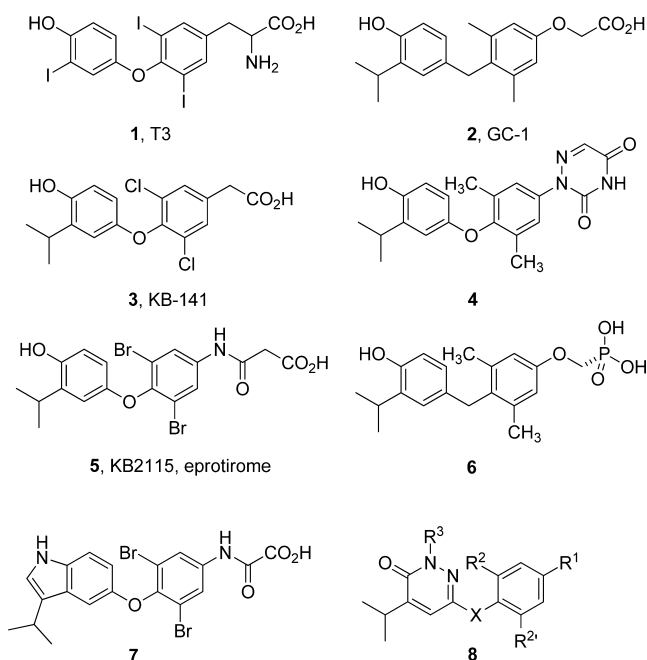
increased rates of atherosclerosis, while excessive levels of thyroid hormone (TH) can lead to adverse effects, particularly in heart and bone. The beneficial metabolic effects of TH are mediated by the thyroid hormone receptor β isoform (THR- β), the predominant liver TH receptor.^{5–8} The adverse heart and bone effects are primarily due to the interaction of TH with the thyroid hormone receptor α isoform (THR- α).^{9–11} Thus, the search for therapeutic agents has focused on finding agonists with selectivity for both the THR- β and the liver. The ligand binding domains of the TH- α and - β receptors differ by only a single amino acid, Asn331 (THR- β)/Ser277 (THR- α), that is capable of making a hydrogen bond with the acidic moiety of **1**. As a result, much of the work on THR- β selective compounds reported to date has focused on close analogues of **1** bearing

Received: December 16, 2013

Published: April 8, 2014

variations in the acidic region capable of selectively interacting with these residues.¹² Chart 1 shows a number of compounds

Chart 1



illustrating the range of TH mimetic structures. GC-1 (**2**)^{6,7} and KB-141⁵ (**3**) represent examples whose pharmacology has been studied extensively. The azauracil **4** represents a further, unusual variation on the acid replacements in the arena of thyroid hormone receptor (THR) mimetics.¹³

A number of THR- β agonists, including **2**, **5** (eprotirome), and a prodrug of **6**, have been evaluated in clinical trials providing validation of their effects on LDL-C and TG lowering. In human clinical studies, once daily oral doses of up to 200 μg of **5** (eprotirome, KB2115) lowered LDL-C by up to 40%,¹⁴ while daily doses of 25–100 μg of **5** given for 12 weeks to patients already receiving statins lowered LDL-C by up to 32%, with no change in thyroid stimulating hormone (TSH) or T3 reported.¹⁵ In a 2-week dose-ascending phase 1 study, a prodrug of **6**, at doses of 2.5 and 5 mg, reduced TG and LDL-C levels by 30% and 15–41%, respectively.¹⁶ However, clinical development of these analogues was discontinued. Some safety issues were noted that included low margins relative to doses that suppress the central thyroid axis, elevated liver enzymes in phase 1 and 2 studies, and in the case of **5**, cartilage damage in preclinical toxicology studies.

In the area of nuclear hormone receptor agonists, it is difficult to predict how subtle alterations in a ligand structure might impact its biological profile. In an effort to identify compounds that were more THR- β selective and potentially safer, we were interested in profiling analogues of T3 that did not contain the very electron rich phenol ring, which was a potential metabolic and safety liability. Indeed, it is reported that in early clinical trials a potentially mutagenic nitrated derivative of **5**, which is thought to be formed by the free radical nitration of the phenolic ring with nitrites at gastric pH, was observed in plasma.¹⁷ A series of patent applications from Bayer describing compounds such as the indole **7** as potent TH agonists illustrated that the T3 phenolic ring could be replaced by a heterocycle.^{18,19} Of several electron deficient heterocyclic

modifications that we investigated, the pyridazinone analogues represented by **8** proved to be the most promising, and this novel heterocycle provided compounds with improved selectivity for THR- β that form the basis of this paper. This work culminated in the identification of MGL-3196 (**53**) which is currently in clinical development.²⁰

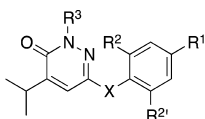
CHEMISTRY

In general, the core bicyclic framework of the compounds shown in Table 1 was prepared by the condensation of the appropriate aryl oxygen, carbon, or sulfur nucleophile with the isopropylidichloropyridazine **11**²¹ followed by functional group transformations as shown in Schemes 1–7. The phenyl acetates **10a** and **10b** were prepared from the corresponding phenols **9a** and **9b** in four steps as shown in Scheme 1 using the general method described by Gardner et al.²² Condensation of the phenols **10a** and **10b** with **11** was effected in the presence of potassium carbonate as the base and a catalytic amount of cuprous iodide in DMSO at 90 °C as generally described by Chen et al.²³ Finally, ester hydrolysis was accomplished under basic conditions and conversion of the chloropyridazines **12a** and **12b** to the corresponding pyridazinones **13** and **14** was carried out by treatment with sodium acetate in acetic acid at 100 °C.²⁴

As shown in Scheme 2, phenyl acetate **15** was chlorinated with sulfuryl chloride followed by reduction with LAH to give dichlorophenol **18a**. The corresponding 2,6-dibromophenols **18b** and **18c** were prepared by bromination of the phenols **16** and **17** with bromine. The key condensation of these compounds with **11** was performed by reaction with potassium *tert*-butoxide in dimethylacetamide at 140 °C overnight in 20–49% yields. Oxidation of the resulting alcohols using Jones reagent (**19a** and **19c**) or 2,2,6,6-tetramethylpiperidin-1-yl)oxy (TEMPO) (**19b**)²⁵ followed by hydrolysis of the chloropyridazine under the conditions noted above provided the 4-substituted 3,5-dihalophenylalkanoic acids **20**–**22**. For the synthesis of *N*-methylpyridazinone **23**, hydrolysis of chloropyridazine **19a** was accompanied by acylation of the primary alcohol. The pyridazinone was methylated with iodomethane in the presence of potassium carbonate, and the acetate was hydrolyzed with sodium hydroxide in methanol. Jones oxidation completed the synthesis of **23**.

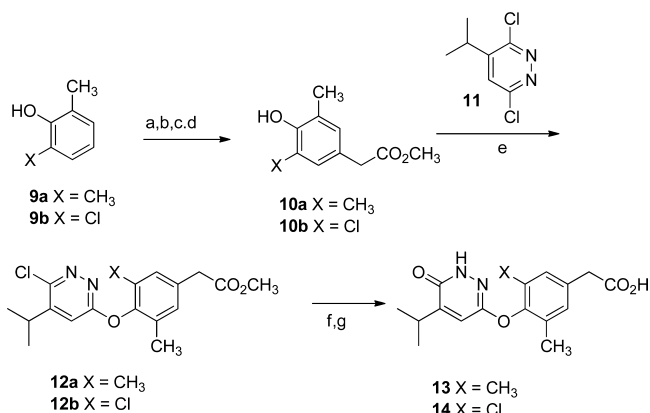
For the synthesis of the glycine and oxamic acid derivatives **26** and **27**, aniline **24** was condensed with **11** under the conditions described in Scheme 1 to give a 50% yield of the ether **25** (Scheme 3). Hydrolysis of the chloropyridazine was accompanied by partial acetylation of the aniline, necessitating a hydrolysis step prior to reductive amination of glyoxylic acid mediated by commercially available resin based MP-cyanoborohydride in the presence of acetic acid to provide **26** directly. Acylation of **25** with methylaloxyl chloride, ester hydrolysis, and hydrolysis of the chloropyridazine provided the oxamic acid **27**.

Schemes 4 and 5 show the preparation of the carbon linked analogues **32** and **38**. Selective displacement of the para-chlorine of nitrobenzene **28** by the anion of *tert*-butyl cyanoacetate provided the alkylated intermediate. Reduction of the nitro group with stannous chloride in ethanolic hydrochloric acid was accompanied by ester hydrolysis and decarboxylation to give aniline **29**.²⁶ Condensation of **29** with **11** followed by hydrolysis provided the pyridazinone **30**. Diazotization of **30** followed by treatment with copper bromide gave the intermediate aryl bromide, which was subjected to

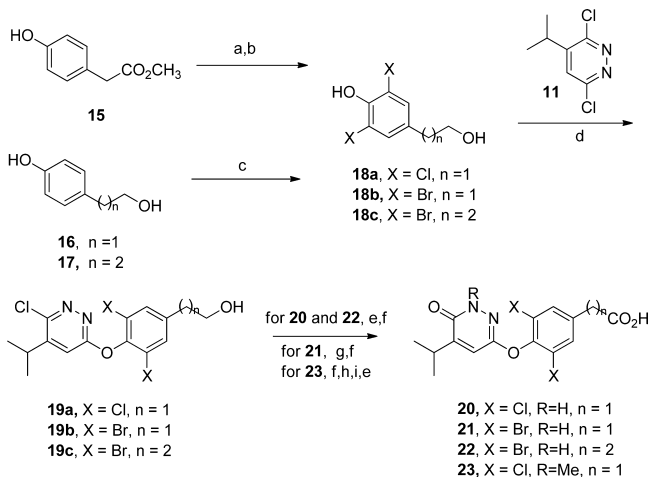
Table 1. Structure–Activity Relationship of Pyridazinone Based TH Agonists^a

Cmpd	R ¹	R ² , R ^{2'}	X	R ³	THR- EC ₅₀ μM ^b	THR-β Rel % Activity of T3	THR- EC ₅₀ μM ^b	THR-α Rel % Activity of T3	Relative Selectivity ^c	MNT
1					0.015 ^d	100.0%	0.01 ^d	100.00%	1	+
2					0.018	126.8%	0.003	83.70%	0.71	-
3					0.023	116.0%	0.005	86.3%	1.02	+
13	-CH ₂ CO ₂ H	CH ₃ , CH ₃	O	H	7.75	24.5%	15.64	19.0%	7.01	+
14	-CH ₂ CO ₂ H	CH ₃ , Cl	O	H	7.01	45.6%	12.00	38.4%	5.90	+
20	-CH ₂ CO ₂ H	Cl, Cl	O	H	2.38	58.2%	7.01	50.0%	10.23	
21	-CH ₂ CO ₂ H	Br, Br	O	H	0.46	80.5%	3.28	54.0%	11.65	+
22	-CH ₂ CH ₂ CO ₂ H	Br, Br	O	H	0.70	89.1%	0.39	97.7%	1.94	
23	-CH ₂ CO ₂ H	Cl, Cl	O	CH ₃	0.77	64.5%	0.78	64.3%	5.51	
26	-NHCH ₂ CO ₂ H	Cl, Cl	O	H	0.67	74.0%	0.70	81.0%	3.66	
27	-NHCOCO ₂ H	Cl, Cl	O	H	0.12	86.9%	0.21	84.4%	6.09	
32	-CH ₂ CO ₂ H	Cl, Cl	CH ₂	H	2.99	57.6%	4.29	59.4%	7.80	
38	-CH ₂ CO ₂ H	Br, Br	CH ₂	H	0.60	74.4%	0.75	72.0%	6.77	
42	-CH ₂ CO ₂ H	Cl, Cl	S	H	2.04	70.4%	8.88	30.2%	7.03	
43	-CH ₂ CO ₂ H	Cl, Cl	SO	H	9.17	9.9%	N/D	N/D	-	
44	-CH ₂ CO ₂ H	Cl, Cl	SO ₂	H	6.98	62.1%	14.39	13.1%	4.15	
53		Cl, Cl	O	H	0.21	83.8%	3.74	48.6%	28.29	-
54		Cl, Cl	CH ₂	H	0.22	87.3%	2.75	46.0%	20.28	-
55		Cl, Cl	O	CH ₃	0.04	93.0%	0.33	64.9%	16.42	
56		Cl, Cl	CH ₂	CH ₃	0.14	90.6%	1.25	64.0%	14.71	
57		Cl, Cl	O	H	0.12	81.3%	0.41	78.4%	12.26	
58		Cl, Cl	CH ₂	H	0.09	91.7%	0.82	67.6%	12.64	

^aN/D is not determined. MNT is in vitro micronucleus test. Superscript b indicates average of triplicate determinations. Superscript c indicates that selectivity is normalized for the selectivity of T3 in the same assay. Superscript d indicates that T3 was run in every assay; the values for THR-β range from 0.12 to 0.024 μM, and the values for THR-α range from 0.003 to 0.10 μM.

Scheme 1^a

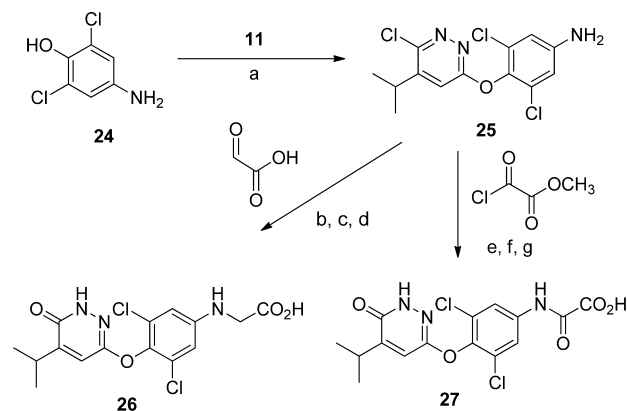
^aReagents and conditions: (a) 40% aq dimethylamine, formaldehyde, EtOH, reflux, 46–66%; (b) (1) iodomethane, ether, (2) NaCN, EtOH, reflux, 55–60% for the two steps; (c) KOH, H₂O, ethylene glycol dimethyl ether, reflux, X = CH₃ 5%, X = Cl, 97%; (d) MeOH, H₂SO₄, 70 °C, 86–91%; (e) **11**, K₂CO₃, CuI, DMSO, 90 °C, 24 h, 67–78%; (f) NaOH, MeOH, 100%; (g) NaOAc, HOAc, 100 °C, 24–48 h, X = CH₃ 65%, X = Cl, 32%.

Scheme 2^a

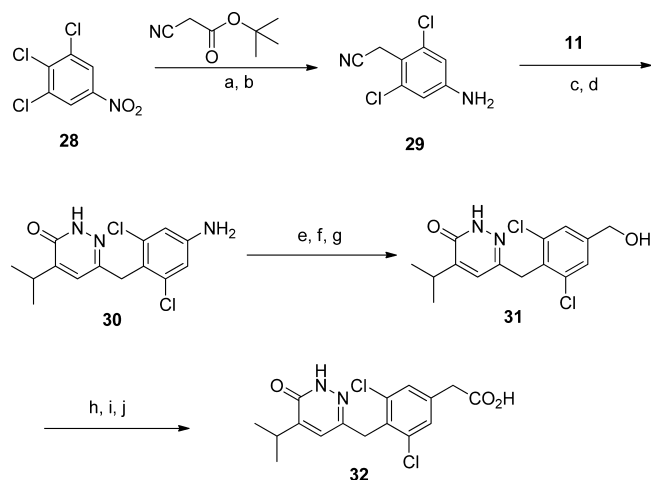
^aReagents and conditions: (a) SO₂Cl₂, diisobutylamine, toluene, 83%; (b) LAH, THF, 100%; (c) (1) Br₂, HOAc; (2) THF, 4 N NaOH, 82–99%; (d) **11**, *t*-BuOK, dimethylacetamide, 140 °C, 24 h, 20–49%; (e) Jones reagent, acetone, 0–10 °C, 95% for **20** and **22**, 19% for **23**; (f) NaOAc, HOAc, 114–120 °C, 24 h, 65–100%, 73% over two steps for **21**; (g) TEMPO, NaClO₂, NaOCl, H₂O, acetonitrile, CH₂Cl₂, Na₃PO₄, pH 6.7, 73%; (h) K₂CO₃, CH₃I, 40 °C, 4 h, then 25 °C, 24 h, 72%; (i) NaOH, MeOH, 25 °C, 24 h, 97%.

palladium-catalyzed carbonylation in methanol followed by treatment with DIBALH in tetrahydrofuran to yield alcohol **31**. Carbon tetrabromide and triphenylphosphine in methylene chloride was used to convert **31** to the corresponding benzyl bromide. Bromide displacement with sodium cyanide²⁷ followed by hydrolysis of the intermediate nitrile gave **32**.

Free radical bromination of methyl 3,5-dibromo-4-methylbenzoate **33** followed by DIBALH reduction of the ester gave the bromomethyl derivative **34**. Displacement of the newly introduced bromine atom with sodium cyanide in DMSO in the presence of sulfuric acid and protection of the primary alcohol as the THP ether afforded the phenylacetonitrile **35**. Condensation of **35** with dichloropyridazine **11** in the presence

Scheme 3^a

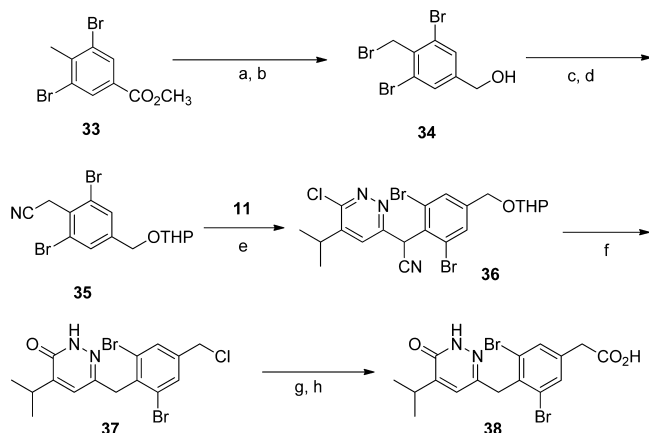
^aReagents and conditions: (a) **11**, K₂CO₃, CuI, DMSO, 90 °C, 24 h, 50%; (b) NaOAc, HOAc, 100 °C, 24 h; (c) 1 N NaOH/MeOH, 100 °C, 24 h, 57% for the two steps; (d) glyoxylic acid, MP-(CN)BH₃, HOAc/MeOH/CH₂Cl₂, MgSO₄, 50 °C, 24 h, 17%; (e) methyloxalyl chloride, DIPEA, THF, 76%; (f) 1 N NaOH, MeOH, 98%; (g) NaOAc, HOAc, 100 °C, 24 h, 56%.

Scheme 4^a

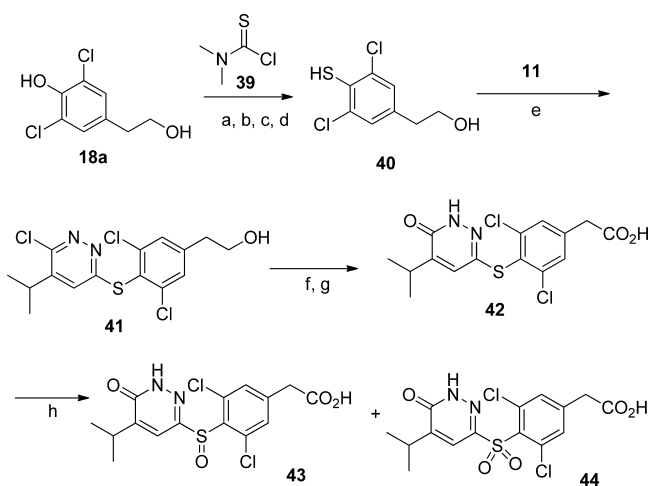
^aReagents and conditions: (a) *tert*-butyl cyanoacetate, K₂CO₃, DMF, 50 °C, 18 h; (b) SnCl₂, EtOH, HCl, 110 °C, 58% (two steps); (c) **11**, *t*-BuOK, THF, 60 °C, 1 h, 77%; (d) HCl/HOAc/H₂O, 120 °C, 24 h, 76%; (e) NaNO₂, H₂SO₄, HOAc, then CuBr/HBr, 100 °C, 51%; (f) Pd(OAc)₂, dppp, Et₃N, CO, MeOH, acetonitrile, 45 psi, 90 °C, 90%; (g) DIBALH, THF, 24 h; (h) CBr₄, PPh₃, CH₂Cl₂, 0 °C, 36% (two steps); (i) NaCN, H₂SO₄, DMSO, 50 °C; (j) HCl, reflux, 13% for the two steps.

of sodium hydride in DMF at 95 °C gave the carbon linked THP-derivative **36**. A related condensation has been reported previously.²⁶ This material was subjected to the standard chloropyridazine hydrolysis conditions followed by treatment with hydrochloric acid in acetic acid at reflux to simultaneously remove the protecting tetrahydropyranyl group and convert the resulting primary alcohol to the corresponding benzylic chloride **37** in 36% yield for the two steps. Conversion of **37** to **38** was carried out in the same manner as the conversion of the benzyl bromide to **32** (Scheme 4).

The sulfur linked analogues **42–44** were available from thiophenol **40**, which was prepared from **18a** (Scheme 6). Coupling of **40** with **11** mediated by potassium carbonate in DMSO gave the pyridazine **41**. Further conversations involved

Scheme 5^a

^aReagents and conditions: (a) NBS, AIBN, CCl₄, reflux, 99%; (b) DIBAL-H, THF, 0 °C, 94%; (c) NaCN, H₂SO₄, DMSO, 78%; (d) dihydropyran, *p*-toluenesulfonic acid, CH₂Cl₂, 85%; (e) **11**, NaH, DMF, 95 °C, 65%; (f) (1) NaOAc, HOAc, reflux, (2) HCl, AcOH, reflux, 36% for the two steps; (g) NaCN, H₂SO₄, DMSO, 60 °C, 67%; (h) HCl, reflux, 49%.

Scheme 6^a

^aReagents and conditions: (a) *t*-Bu(Ph)₂SiCl, Et₃N, CH₂Cl₂, 60%; (b) **39**, DABCO, DMF, 90%; (c) 198 °C, 70%; (d) 3 N KOH, EtOH, 95 °C, 76%; (e) **11**, K₂CO₃, DMSO, 90 °C, 52%; (f) Jones reagent, acetone, 0 °C, 89%; (g) HOAc, NaOAc, 100 °C, 17%; (h) 30% H₂O₂, HCO₂H, 0 °C, 41% **43** and 27% **44**.

hydrolysis and Jones oxidation to provide **42**. Oxidation of **42** with 30% hydrogen peroxide in formic acid at 0 °C gave a separable mixture of the sulfoxide **43** and sulfone **44**.

Scheme 7 outlines the preparation of the oxygen and carbon linked azauracils **53**–**58**. For the synthesis of the intermediate *N*-methylpyridazinones **46** and **47**, it was necessary to protect the starting anilines as their phthalimides prior to methylation with dimethylformamide dimethyl acetal using a procedure described by Sotelo et al.²⁸ The general procedure described by Carroll et al.²⁹ was employed to prepare intermediates **49**–**52** by sequential diazotization of anilines **30** and **45**–**47** followed by treatment of the resulting diazonium salt with cyanoacetylurethane **48**. Cyclization of the crude product was effected by treatment with sodium acetate in acetic acid at 120 °C to provide the targeted cyanoazauracils. Removal of the nitrile to

give the azauracils **57** and **58** was accomplished in two steps by hydrolysis to the corresponding acid mediated by hydrochloric acid in acetic acid at reflux and decarboxylation by means of treatment with mercaptoacetic acid at elevated temperature.²⁹

RESULTS AND DISCUSSION

Activity in in Vitro Functional Assays. Most of the selectivity reported for thyromimetics in the literature is derived from assessment of the compound's relative binding affinities for THR- β and THR- α . While this information is useful, it does not provide information on their ability to act as agonists. Thus, we decided to implement an in vitro functional assay as a potentially more relevant indicator of selectivity. A cell free coactivator recruitment assay was developed for both THR- β and THR- α , providing information on the functional potency and selectivity of analogues. In this assay, T3 or compound is allowed to bind to his-tagged THR in the presence of RXR. The ability of this liganded heterodimeric complex to recruit biotin-linked coactivator peptide GRIP1 (SRC-2) is measured with FRET. The activity of the compounds described above for THR- β and THR- α is reported in Table 1. The selectivity reported for each compound is normalized for the selectivity of T3 run in the same assay.

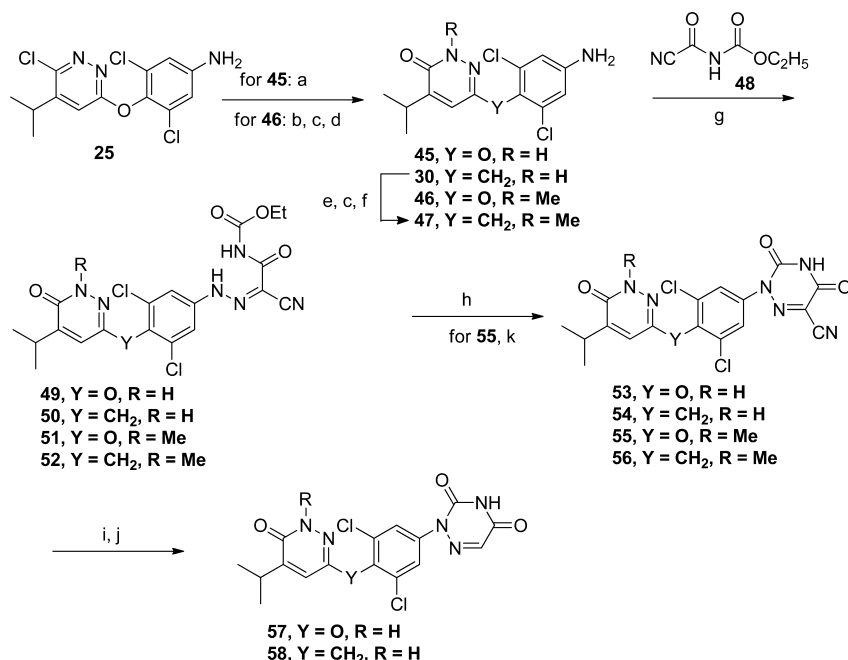
Two well-studied compounds, **2** and **3**, have been reported to be 10-fold³⁰ and 14-fold³¹ β selective, respectively, in binding assays. These compounds were unselective in the coactivator recruitment assay. In a reporter cell assay,³¹ **3** was only 3-fold β selective, which illustrates that the selectivity in binding and functional assays can be quite different. While **5** and **6** were not tested in our assay, **5** is reported to have "modestly higher" THR- β selectivity,¹⁵ and **6** was reported to be 12-fold selective in a binding assay,³² suggesting that these analogues did not have high THR- β selectivity.

Replacement of the phenol of **3** with a pyridazinone gave **20** which was 10-fold more selective for THR- β than **3**. While **20** was 100-fold less potent than **3** (2.38 μ M versus 0.023 μ M), the potency was good enough to provide a reasonable starting point for optimization of this series directed toward improving potency and selectivity. Replacing one or both of the chlorines with methyl (**13**, **14**) resulted in a slight loss of both potency and selectivity. On the other hand, the dibrominated analogue **21** was 5-fold more potent and equally as selective as **20**.

Replacing the oxygen linker of analogues **20** and **21** with a methylene linker gave compounds **32** and **38** that were comparable in potency but somewhat less selective. The sulfur, sulfoxide, and sulfone linkers (**42**–**44**) were all less selective than the oxygen linker. While the dibrominated analogues are more potent than the dichlorinated analogues, concerns about the general safety of aromatic brominated compounds led us to focus on the dichlorinated analogues.

Modification of the acetic acid substituent potentiates the potency and selectivity of the compounds. The propionic acid analogue **22** was 6-fold less selective than the acetic acid analogue **21**. The amino acetic acid and amino oxalic acid analogues **26** and **27** were more potent, but less selective, than **20**.

A large increase in potency was obtained when the acyclic acidic groups were replaced with an azauracil. Azauracil **57** was 20-fold more potent than **20** and slightly more selective. A further increase in selectivity was obtained by substituting the azauracil with a cyano group. This substituent increased the selectivity from 12-fold (**57**) to 28-fold (**53**) with minimal impact on potency (**53**, 0.21 μ M; **57**, 0.12 μ M). As with the

Scheme 7^a

^aReagents and conditions: (a) (1) NaOAc, HOAc, H₂O, 100 °C, 1.5 h, (2) NaOH/MeOH, 57%; (b) (1) phthalic anhydride, toluene, reflux, (2) NaOAc, HOAc, H₂O, 120 °C, 68%; (c) DMF dimethyl acetal, 100 °C, 52–73%; (d) butylamine, methanol, reflux, 1.5 h, 74%; (e) phthalic anhydride, HOAc, 130 °C, 61%; (f) HOAc, 110 °C, 69%; (g) (1) NaNO₂, HCl, 0 °C, (2) 48, pyridine, H₂O, 0 °C, 76–95%; (h) NaOAc, HOAc, or KOAc, DMA 120 °C, 1.5–3.5 h, 44–86%; (i) HCl, HOAc, 120 °C, 48 h, 78%; (j) mercaptoacetic acid, 170 °C, 1 h, 23–40%; (k) dimethylacetamide, KOAc, 120 °C, 2 h, 86%.

acyclic acid substituted compounds, the methylene linked azauracils **54** and **58** were roughly comparable in potency but slightly less selective than the corresponding analogues with an oxygen linker (**53** and **57**).

For T3 and other TH agonists, a key structural feature has been the presence of phenol or an alternative hydrogen bond donor to interact with histidine 435. Methylation of the pyridazinone nitrogen provides derivatives with no possibility of acting as hydrogen bond donors. Remarkably, the methylated analogues **23**, **55**, and **56** are more potent, although less selective, than the corresponding protonated analogues **20**, **53**, and **54**. For the methylated analogues, and possibly for all the pyridazinone compounds, histidine 435 may be serving as a hydrogen bond donor to the pyridazinone carbonyl.

In addition to the IC₅₀ values, the level of maximum activity is reported in Table 1 as the percentage of the maximum activity of each analogue relative to the maximum efficacy of T3. It is interesting to note that while **2** and **3** achieved higher activity than T3, all of the pyridazinone agonists had less than 100% activity. This is another indication of the differences between the pyridazinone series and earlier analogues.

Early pyridazinone compounds **13**, **14**, and **21** substituted with an acetic acid side chain were positive in an in vitro micronucleus assay, as were **3** and T3 (**1**). Eliminating this activity was one of the goals of the program. We were pleased to find that the cyanoazauracils **53** and **54** were not only more potent and selective than the acetic acid analogues but were also negative in this assay.

Modeling. We modeled the binding of the cyanoazauracil analogues with THR-β. Of the many published cocrystal structures of THR-β, the structure with the most similar bound ligand is PDB structure 1N46.¹³ This structure includes the THR-β ligand binding domain together with the TH mimetic

(**4**) that incorporates a bound azauracil in place of the carboxylic acid moiety found in most ligands for this target. In order to construct a model for the pyridazinones bound to THR-β, we modified **4** to construct **53**. This structure was then submitted to limited optimization, providing a very conservative model for **53** bound to THR-β (Figure 1), shown with T3 (from 3GWS)³³ superimposed.

The cyano group in **53** was easily accommodated in the 1N46 active site with little induced movement of the active site residues (Figure 1). Indeed the cyano group appears well

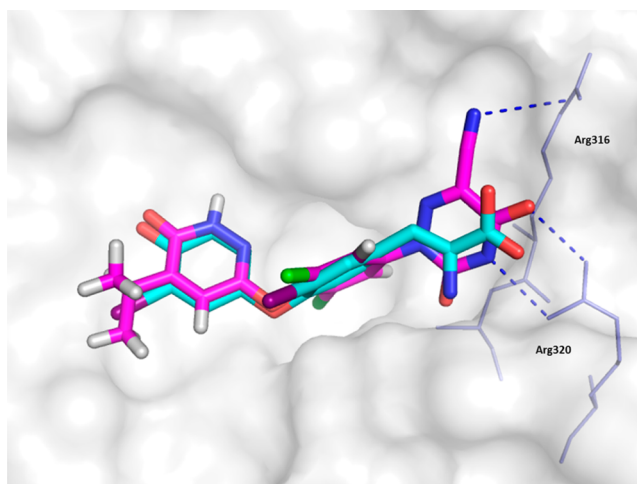


Figure 1. Model of **53** (magenta) bound to THR-β (1N46) with the T3 geometry (cyan) from 3GWS superimposed. Polar interactions of **53** in the anion binding site are highlighted.

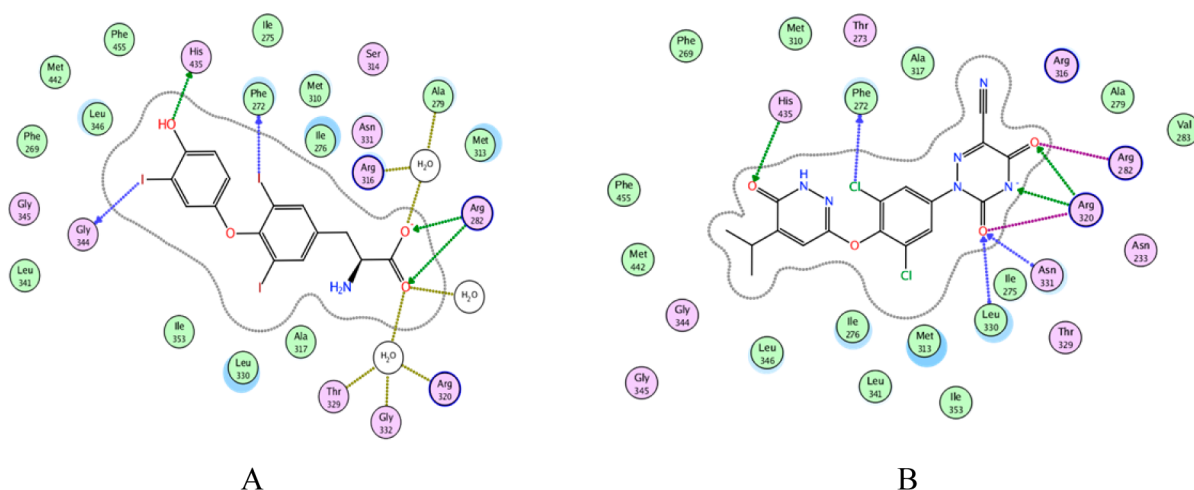


Figure 2. (A) 2D description of the binding site for T3 (PDB code 3GWS). (B) 2D description of the binding site for the 53 model (MOE).

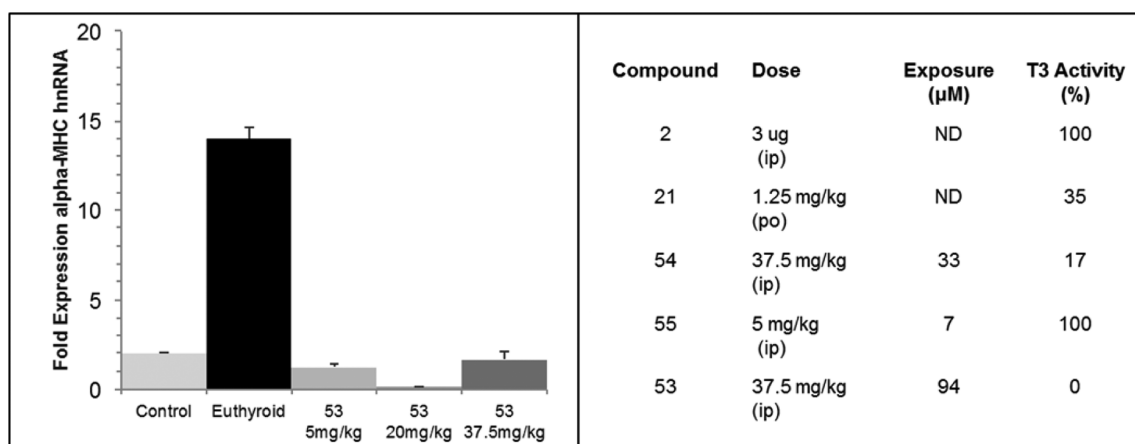


Figure 3. Left panel: cardiac α -MHC hnRNA relative levels (arbitrary units) in untreated thyroidectomized rats (control), euthyroid rats, and thyroidectomized rats 6 h after exposure to 53 dosed intraperitoneally at the specified doses.³⁵ Right panel: activities of tested compounds relative to full activity (euthyroid or T3-treated) and exposure of the compound 6 h after dose. ND is not determined.

positioned to pick up an additional interaction with Arg316 (Figures 1 and 2).

Modeled 53 binds in a fashion that is very similar to T3. As can be seen from the 2D projections (Figure 2), the T3 interactions with the positively charge ARG320 are mediated by a series of bridging waters. In the model, as in the azauracil analogue crystal structure (1N46), the cyanoazauracil of 53 interacts directly with ARG320. The large more diffuse negatively charged heterocycle in 53 may convey advantages over the conventional acids, since it displaces several waters and would be expected to suffer a smaller binding desolvation penalty relative to a carboxylic acid.³⁴

Cardiac-Specific Effects of a Single Dose of 53 in Adult Male Sprague–Dawley Rats. An important feature of a selective TH mimetic is avoiding cardiac effects, which are largely mediated by THR- α receptors. The purpose of this study was to determine the effect of 53 on the expression of the α -myosin heavy chain (α -MHC) gene in the hearts of rats that are hypothyroid because of surgical removal of the thyroid. α -MHC expression is up-regulated by the activation of the THR- α . Since hypothyroid rats express very low levels of α -MHC compared to euthyroidic rats, α -MHC expression in hypothyroidic rats is a sensitive marker for TH regulated gene expression in the heart. Treatment of these thyroidectomized

rats with T3 restores the level of gene transcription to euthyroid-like levels.

Expression of α -MHC hnRNA after treatment with low, medium, and high doses of 53 ip is shown in Figure 3. Compound 53 was given at 5, 20, and 37.5 mg/kg, ip, to yield six hour postdose plasma concentrations of 15.4, 57, and 94 μM , respectively, and remarkably showed little to no induction of α -MHC hnRNA. The data suggest that 53, compared to T3 or literature analogues such as 2, has little effect in the rat heart as measured by changes in α -MHC levels (Figure 3, right panel).³⁵

The acetic acid analogue 21, dosed orally, had 35% of the T3 activity at reasonably low exposures. The methylene linked cyanoazauracil analogue 54 (dosed ip) had no effect at the two lowest concentrations tested but did demonstrate a small but significant increase in α -MHC transcription to 17% of euthyroid levels at the highest concentration tested (37.5 mg/kg).³⁵ By contrast, the N-methylated analogue 55 (dosed ip) induced full agonist activation of α -MHC transcription of the cardiac-specific gene α -MHC at all doses tested. Even at the lowest dose tested (5 mg/kg), transcription was measured at euthyroid levels.

Several factors, including heart uptake and THR- α activity, impact the performance of compounds in this assay.

Table 2. Selected Property Data for 53

% free (human)	human hepatocyte, CL _{int} ((μ L/min)/10 ⁶ cells)	hERG, IC ₂₀ (μ M)	CYP inhibition, IC ₅₀ (μ M)	CYP TDI 3A4/5, 2C9, 2C19	solubility, pH 7.04 (μ M)	Caco-2 A–B (1 \times 10 ⁻⁶ cm/s)	Caco-2 efflux ratio
0.6	1.04	~30	3A4/5: >50 2C19: >50 2C9: ~22	none detected	1.0	1.37	18.4

Compound **53** was the only analogue with no activity at high exposure and was selected for further evaluation.

In Vitro and in Vivo Profiling of 53. Compound **53** showed low clearance and high stability in cryopreserved human hepatocytes (Table 2). In Caco-2 cells, **53** displayed low to medium-low permeability in the apical (A) to basolateral (B) direction and high permeability in the B to A direction. In addition, a liver to plasma ratio of 8:1 was observed for **53** in diet induced obese (DIO) mice.³⁶ Since the metabolic efficacy of **53** is due to its effects in the liver, its concentration in the liver coupled with the reasonably low permeability should contribute to the safety of the compound by reducing systemic exposure. This is especially important for limiting uptake to the pituitary, where THR- β is responsible for central thyroid axis regulation.

Compound **53** showed an IC₂₀ of roughly 30 μ M for blockage of the hERG channel (Table 2). The IC₅₀ for CYP3A4/5 and for CYP2C19 was >50 μ M, the highest concentration tested, and there was only weak inhibition (roughly 22 μ M) of CYP2C9. In the presence or absence of NADPH, no time dependent inhibition (TDI) of any of these CYP enzymes was observed.

When dosed as a suspension, **53** exhibited good exposures and reasonable oral bioavailability in rats (Table 3). The volume of distribution and clearance were both low. Dose proportional increases in exposure were observed for a suspension of **53** given orally to DIO mice.³⁶

Table 3. Pharmacokinetic Parameters of 53 after iv and po Administration to Rats (Mean Values, N = 3, SD in Parentheses)

route	rat	
	iv	po
dose (mg/kg)	5	5
AUC (μ g·h/mL)	38.1(11.4)	17.4(8.6)
T _{max} (h)		6(0)
C _{max} (μ g/h)		1.71(0.85)
CL (mL min ⁻¹ kg ⁻¹)	2.35(0.85)	
V _{ss} (L/kg)	0.422(0.057)	
T _{1/2} (h)	3.4(0.26)	4.08(1.16)
F (%)		45(22.5)

In a 23-day study of **53** in C57Bl/6J-diet-induced obese (DIO) mice, animals were treated with daily oral doses of either **53** vehicle control or 0.3, 1.0, 3.0, or 10 mg/kg **53**. In a parallel 24-day study using identical age DIO mice and identical protocol design, mice were treated with either T3-vehicle control or 10, 30, or 100 μ g/kg T3. At the end of the study, laboratory assessments and body composition measurements were made. In animals treated with **53** there was a reduction in cholesterol and in liver size, which is secondary to reduction of liver TG.³⁶ There was no effect on bone mineral density (BMD) or heart or kidney size (data not shown) in **53** treated animals. By contrast, while T3 treated animals demonstrated

cholesterol lowering, there was no effect on liver size. A significant increase in heart and kidney size (data not shown) accompanied by significant decreases in BMD of 10–13% was observed at all doses of T3 (Figure 4).

Compound **53** was evaluated in a number of additional animal models.³⁶ In both hypercholesterolemic rat and rabbit models, **53** significantly lowered non-HDL-C and liver TG at doses where, when assessed, there was no effect on TSH levels or the central thyroid axis. In the rabbit model, there were indications of an additive lipid lowering effect when **53** was coadministered with atorvastatin. Additionally, in a DIO mouse study, **53** improved insulin sensitivity and lowered glucose to a near normal level.

First in Human Studies. The safety profile and tolerability of **53** were assessed in humans in a single ascending dose study followed by a 2-week multiple dose study.²⁰ In the multiple ascending dose study, healthy subjects with mildly elevated LDL-C (>110 mg/dL) received once daily oral doses of **53** ranging from 5 to 200 mg. Compound **53** was safe and well-tolerated at all doses tested with no drug-related adverse events. There was no evidence of central thyroid axis dysfunction at any dose, no effect on heart rate, QT interval, or vital signs, and no effect on liver enzymes.

At the highest doses of **53** reversible dose-related reductions in free T4 of ~20% (200 mg) and ~10% (100 mg) were observed. Free T3 and TSH showed no meaningful or dose-dependent change compared with placebo, indicating that this is not an effect on the central thyroid axis. This change, which is not of a magnitude that is clinically meaningful, may be attributed to increased hepatic THR- β agonism leading to increases in the level of hepatic deiodinase 1, which reduces the level of the prohormone T4 and has no effect on the metabolism of the active T3.²⁰ Similar observations were made in preclinical studies.³⁶

Drug exposure in the plasma increased with increasing dose. The increase in exposure was fairly linear through 80 mg, with higher variability at the higher doses.

While the primary purpose of these studies was assessment of safety, effects on lipids were observed in the multiple ascending dose study. Statistically significant reductions relative to placebo of up to 30% for LDL-C and statistical trends of up to 60% reduction in TG were observed for doses ranging from 50 to 200 mg. The near maximal lipid effects were observed at a dose of 80 mg daily.

CONCLUSION

Our efforts to identify selective THR- β agonists that did not contain the highly electron-rich phenolic moiety characteristic of other TH mimetics led to the identification of a pyridazinone series. The initial compounds were significantly less potent and more selective than previously reported compounds **2** and **3**. Replacement of the acetic acid substituent with a cyanoazauracil improved both the potency and selectivity of the compounds, leading to **53** which is 28-fold selective for THR- β over THR- α in an in vitro functional coactivator recruitment assay.

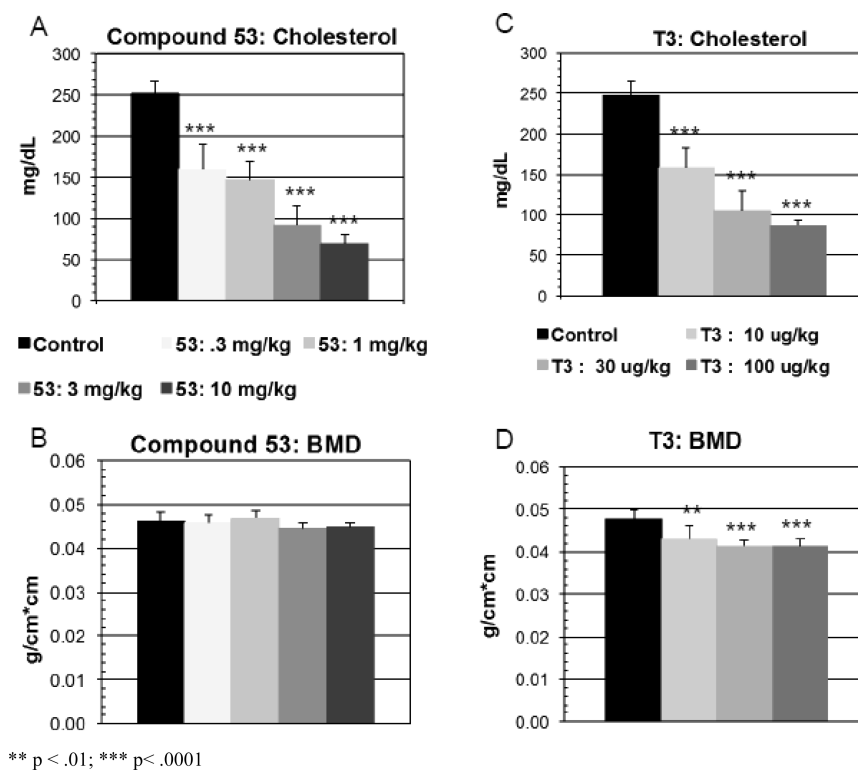


Figure 4. Effects of 53 vs T3 on cholesterol and BMD in DIO mice.

Compared with all other compounds tested, **53** showed no THR- α mediated gene expression in a rat heart model. In vitro assays are predictive of low potential for off target actions. Despite the low to medium permeability and potential for efflux observed in the Caco-2 assay, **53** has demonstrated reasonable plasma exposures in preclinical animal models and in humans. The permeability and potential for efflux coupled with selective uptake into the liver may contribute to the safety of **53** by minimizing thyroid actions outside the liver. When dosed orally to DIO mice, **53** reduced cholesterol levels and liver size without the side effects observed with T3 of decreased BMD and increased heart and kidney size. In healthy volunteers, **53**, at once daily oral doses of 50 mg or higher for 2 weeks, exhibited an excellent safety profile, significantly decreased LDL-C by up to 30%, and showed a statistical trend to reduce TG up to 60%.²⁰ Future investigations, including clinical trials, will assess the safety and test the ability of **53** to treat patients, including diabetics, with mixed dyslipidemias and/or NAFLD and NASH both as a single agent and in combination with statins.

EXPERIMENTAL SECTION

All nonaqueous reactions were carried out under an argon or nitrogen atmosphere at room temperature unless otherwise noted. All reagents and anhydrous solvents were used as obtained commercially without further purification or distillation unless otherwise stated. Analytical thin-layer chromatography (TLC) was performed on EMD Chemicals silica gel 60 F254 precoated plates (0.25 mm). Compounds were visualized by UV light and/or stained with either *p*-anisaldehyde, iodine, or phosphomolybdic acid or KMnO₄ solutions followed by heating. Analytical high-pressure liquid chromatography (HPLC) and LC-MS analyses were conducted using the following two instruments and conditions. Method 1 involved the following: Hewlett-Packard HP-1090 pump and HP-1090 PDA detector set at 215 nm with the MS detection performed with a Micromass Platform II mass

spectrometer with electrospray ionization (ESI); Chromegabond WR C18 3 μ m, 120 \AA , 3.2 mm \times 30 mm column; solvent A, H₂O–0.02% TFA; solvent B, MeCN–0.02% TFA; flow rate, 2 mL/min; start 2% B, final 98% B in 4 min, linear gradient. Method 2 involved the following: Waters 2795 pump and Waters 2996 photodiode array detector set at 214 nm with the MS detection performed with a Waters ZQ mass spectrometer (ESI); Epic Polar hydrophilic 3 μ m, 120 \AA , 3.2 mm \times 30 mm column; solvent A, H₂O–0.03% HCO₂H; solvent B, MeCN–0.03% HCO₂H; flow rate, 2 mL/min; start 10% B, final 100% B in 3 min linear gradient, remaining for 1 min. All final compounds reported were analyzed using one of these analytical HPLC methods and were at least 95% pure.

Flash column chromatography was performed on EM Science silica gel 60 or with prepacked Biotage or Isco silica gel columns. Preparative reverse-phase high-pressure liquid chromatography (RP-HPLC) used a Waters Delta prep 4000 pump/controller, a 486 detector set at 215 nm, and a LKB Ultrac fraction collector on a C-18 column using acetonitrile/water with 0.1% TFA. ¹H NMR spectra were recorded using a Varian Mercury 300 MHz or Varian Inova 400 MHz spectrometer. The chemical shifts are in parts per million (δ) referenced to Me₄Si (0.00 ppm) or CHCl₃ (7.26 ppm). High-resolution mass spectra were recorded on a Bruker Apex II FTICR mass spectrometers with a 4.7 T magnet (ES) or Micromass AutoSpec (EI) mass spectrometers.

6-(4-Amino-2,6-dichlorophenoxy)-4-isopropyl-2H-pyridazin-3-one 45. A mixture of glacial acetic acid (30 mL), sodium acetate (860 mg, 10.5 mmol), and **25** (1.0 g, 3.0 mmol) was heated to 100 °C for 24 h. The reaction mixture was cooled to room temperature, stirred for 2 days, and concentrated. The residue was diluted with water (200 mL) and was made basic to pH 9 by the addition of 1 N sodium hydroxide solution. The suspension formed was extracted with ethyl acetate (1 \times 250 mL). The water layer was acidified to pH 5 by the addition of concentrated hydrochloric acid. The water layer was extracted with ethyl acetate (1 \times 250 mL). The organic layers were combined, dried with magnesium sulfate, filtered, and concentrated under vacuum. The resulting oil was diluted with methanol (20 mL) and was treated with a 1 N aqueous sodium hydroxide solution (20 mL, 20 mmol). The reaction mixture was

heated to 120 °C for 24 h. The reaction mixture was cooled to room temperature, and the solvent was concentrated under vacuum. The residue was diluted with water (100 mL) and was extracted with ethyl acetate (200 mL). The ethyl acetate layer was washed with water containing a 1 N aqueous hydrochloric acid solution (to pH 5) and saturated sodium chloride solution, dried with magnesium sulfate, filtered, and concentrated under vacuum. The residue was dissolved in chloroform and purified by flash chromatography (Biotage 40L) using silica gel, eluting with a 1:1 ethyl acetate/hexanes solution with 0.5% glacial acetic acid. The desired fractions were collected and concentrated under vacuum and dried under high vacuum at 37 °C. The solid was slurried in diethyl ether (~10 mL) and petroleum ether (10 mL). The solid was stirred for 20 min at room temperature, filtered, and rinsed well with petroleum ether. The solid was dried under high vacuum to afford **45** (538 mg, 57%) as an off-white solid. LRMS for $C_{13}H_{13}Cl_2N_3O_2$ ($M + H$)⁺ $m/z = 314$.

Ethyl (2-Cyano-2-(2-(3,5-dichloro-4-(5-isopropyl-6-oxo-1,6-dihydropyridazin-3-yl)oxy)phenyl)hydrazono)acetyl)-carbamate 49. A suspension of **45** (134 mg, 0.42 mmol) in water (5.6 mL) was treated with concentrated hydrochloric acid (2.8 mL). The reaction mixture was cooled to 0 °C and was treated with a solution of sodium nitrate (36.5 mg, 0.529 mmol) in water (0.2 mL) under the surface of the reaction mixture followed by a water (0.2 mL) rinse. The reaction mixture was stirred at 0 °C for 30 min, and a solution formed. In a separate flask, equipped with a magnetic stirrer, were added **48** (73 mg, 0.46 mmol), water (9.4 mL), and pyridine (2.8 mL). This mixture was cooled to 0 °C, and the solution from the first reaction was quickly filtered and poured into the second reaction mixture. An orange precipitate formed, and the suspension was stirred at 0 °C for 30 min. The solid was filtered and rinsed with water followed by petroleum ether. Drying in a vacuum oven overnight at 80 °C afforded **49** (156 mg, 76%) as an orange solid. EI(+)-HRMS m/z calcd for $C_{19}H_{18}Cl_2N_6O_5$ ($M + H$)⁺ 481.0789, found 481.0790.

2-[3,5-Dichloro-4-(5-isopropyl-6-oxo-1,6-dihydropyridazin-3-yloxy)phenyl]-3,5-dioxo-2,3,4,5-tetrahydro[1,2,4]triazine-6-carbonitrile 53. A mixture of **49** (3.49 g, 7.17 mmol) in glacial acetic acid (72 mL) was treated with sodium acetate (2.94 g, 35.8 mmol) at room temperature. The reaction mixture was heated to 120 °C for 1.5 h. At this time, the reaction mixture was cooled to 0 °C, diluted with water (220 mL), and stirred for 30 min. The resulting solid was filtered and rinsed with water (3 × 100 mL) followed by petroleum ether (3 × 100 mL). The solid was air-dried for 30 min. The solid was dissolved in hot acetonitrile (250 mL). The resulting red mixture was treated with neutral decolorizing carbon, filtered through Celite, and rinsed with acetonitrile (1 L) until no further UV active material eluted. The yellow filtrate was concentrated under reduced pressure. The resulting solid was triturated with hot acetonitrile (50 mL), cooled for 15 min, diluted with water (100 mL), and filtered. The solid was triturated again with hot acetonitrile (10 mL), filtered, and rinsed with acetonitrile, water, and petroleum ether. The solids were collected and dried under high vacuum overnight and then dried in a vacuum oven at 80 °C overnight to afford **53** (1.91 g, 61%) as a yellow solid. ¹H NMR (400 MHz, DMSO-*d*₆) δ 13.28 (br s, 1H), 12.24 (s, 1H), 7.78 (s, 2H), 7.45 (s, 1H), 2.94–3.17 (m, 1H), 1.20 (d, *J* = 6.82 Hz, 6H). EI(+)-HRMS m/z calcd for $C_{17}H_{12}Cl_2N_6O_4$ ($M + H$)⁺ 435.0370, found 435.0368.

THR/RXR/GRIP1 Assay. The ligand binding domain (amino acids 148–410) of THR-β (H6-THR-β) and the ligand binding domain (amino acids 202–461) of THR-α (H6-THR-α) were cloned into an *E. coli* expression vector pET28a (Novagen, Milwaukee, WI) that contained a N-terminal hexa His sequence. The resulting recombinant hexa His tagged proteins were produced in *E. coli* BL21(DE3) cells. Cells were grown in Terrific Broth (in-house prepared medium of Bacto tryptone (3.3%, w/v), Difco yeast extract (2.0%, w/v), and NaCl (0.5%, w/v)) using shake flasks with a 24 h induction in 0.2 mM IPTG at 25 °C, harvested, and lysed with five volumes of buffer A (0.05 M Tris, 0.3 M NaCl, 1%W/V betaine, 0.01 M imidazole, 0.02 M β-mercaptoethanol, pH 8.0). Lysozyme (1.0 mg/mL, Sigma) and Complete protease inhibitor cocktail (Roche Diagnostics GmbH) were added to slurry, and the solution was sonicated for 1 min five times at

4 °C. The suspension was centrifuged in a Ti45 Beckmann rotor for 2 h at 127 300 RCF, and the supernatant was loaded onto NI_NTA agarose (Quigen 30210) column. After a washing with buffer A, H6-TRβ or H6-TRα was eluted with buffer A containing 0.25 M imidazole.

The ligand binding domain of human retinoid X receptor (amino acids 225–462) (RxRα) was engineered with N-terminal His6 and EE (EFMPME) tags, a thrombin cleavage site between the His6 and EE sequences, and cloned into pACYC vector. The resulting His6-EE-tagged protein was produced in *E. coli* cells. Cells were grown using shake flasks with an 18 h induction in 0.1 mM IPTG at 18 °C, harvested, and suspended with five volumes of buffer B (0.025 M Tris, 0.3 M NaCl, 0.02 M imidazole, 0.01 M β-mercaptoethanol, pH 8.0). Lysozyme (0.2 mg/mL, Sigma) and Complete protease inhibitor cocktail (Roche Diagnostics GmbH) were added and stirred for 30 min at 4 °C. The suspension was sonicated for 30 s, five times, at 4 °C. The suspension was centrifuged for 20 min at 12 000 RCF. The supernatant was filtered by 0.45 μm pore size membrane, and 0.5% NP-40 was added. The His6-tagged protein was bound to and eluted from NiNTA metal-affinity resin (QIAGEN, Valencia, CA). The protein was concentrated and dialyzed.

The His6 tag was removed from EE-RxRα by thrombin digestion, using 10 units of thrombin (Pharmacia, Piscataway, NJ) per milligram of protein and incubating for 2 h at 25 °C. Removal of thrombin was done batchwise using benzamide-Sepharose 6B (Pharmacia, Piscataway, NJ). The protein was concentrated and dialyzed. This protein was used in the coactivator peptide recruitment assay.

Europium-conjugated anti hexa His antibody and APC-conjugated streptavidin were purchased from PerkinElmer Life and Analytical Sciences.

THR-β/RXR/GRIP1 Coactivator Peptide Recruitment Assay.

An amount of 30 μL of H6-THR-β (50 nM) in 50 mM Hepes, pH 7.0, 1 mM DTT, 0.05% NP40, and 0.2 mg/mL BSA (binding buffer) was mixed with an equal volume of EE-RxRα (50 nM) in binding buffer. An amount of 6 μL of T3 (0–14.8 μM) or test compound (0–1.2 mM) in DMSO was then added and the solution incubated at 37 °C for 30 min. Then 30 μL of biotin-GRIP1 peptide (biotin-Aca-HGTSLSKEKHILHRLQLDSSSPVDL-CONH₂) (100 nM) in 30 μL of binding buffer plus 5% DMSO was added and the solution incubated at 37 °C for 30 min. An amount of 30 μL of solution containing 12 nM europium-conjugated anti hexa His antibody and 160 nM APC-conjugated streptavidin in 50 mM Tris, pH 7.4, 100 mM NaCl, and 0.2 mg/mL BSA was added, and the solution was incubated at 4 °C overnight. An aliquot (35 μL/sample) was transferred to 384-well black microtiter plates. The HTRF signal was read on the Victor 5 reader (PerkinElmer Life and Analytical Sciences).

THR-α/RXR/GRIP1 Coactivator Peptide Recruitment Assay.

The assay protocol is essentially the same as that of THR-β/RXR/GRIP1 coactivator peptide recruitment assay as described above except that 125 nM H6-THR-α, 125 nM EE-RxRα, and 250 nM biotin-GRIP1 were used.

Computational Procedure. Analyses of the crystal structures and computer graphics were done using PyMol.³⁷ The structure for **53** was constructed by manually modifying the crystal structure of the azaracil derivative **4**. The resulting structure was then submitted to limited optimization using the MMFF force field³⁸ with the protein structure frozen, followed by additional optimization using the LigX capability in MOE.³⁹ The ligand was given a formal charge of –1, and the protonation states for the protein were assigned using MOE. The protein atoms were restrained during optimization with all atoms falling beyond 6 Å being frozen. This resulted in a model for **53** bound to the receptor where the protein structure is little changed from PDB code 1N46.¹³

Thyroidectomized Rat Cardiac Myocyte Assay. These assays were conducted under the direction of Irwin Klein using the previously described procedures.³⁵ Compounds **53**, **54**, and **55** were formulated in 4% DMSO, 15% PEG-400, and 81% of 30% HPBCD in phosphate buffer and were administered intraperitoneally. For **53** and **54**, 4 rats per group were tested at 5, 20, and 37.5 mg/kg. For **55**, 3 rats per group were tested at 5 and 15 mg/kg and 4 rats were tested at 50 mg/kg

kg. Compound **21** was formulated in 2% Klucel LF, 0.1% Tween 80, water and dosed orally ($n = 3$ per group) at 0.0625, 0.25, and 1.25 mg/kg.

C57Bl/6J-Diet-Induced Obese (DIO) Mice Study. All animal studies were done according to IACUC approved protocols. Six week old C57Bl/6J mice were placed on a high fat diet for 34 weeks. At day 0, 9 mice per group were treated daily doses by gavage with vehicle (2% Klucel LF, 0.1% Tween 80 in water) or 0.3, 1, 3, or 10 mg/kg **53** for 23 days. In a parallel study, at day 0, 9 mice per group were treated with daily doses of vehicle (Dulbecco's phosphate buffered saline, pH adjusted to 9.0 with 1 N NaOH) or 10, 30, or 100 $\mu\text{g}/\text{kg}$ T3. Body weight and food intake were monitored during the study. BMD and body composition assessments were made on day 22. On day 23 at necropsy, organ weights were obtained for determination of organ weight and blood samples were assessed for cholesterol and other chemistry parameters.

■ ASSOCIATED CONTENT

● Supporting Information

Synthetic procedures and analytical data for all compounds except for **53**; procedures for in vitro tests. This material is available free of charge via the Internet at <http://pubs.acs.org>.

■ AUTHOR INFORMATION

Corresponding Author

*Phone: 267-327-4448. E-mail: martha@madrigalpharma.com.

Notes

The authors declare the following competing financial interest(s): M. Kelly and R. Taub are employed by Madrigal Pharmaceuticals.

■ ACKNOWLEDGMENTS

We thank Joseph Grimsby and Dennis Kertesz for helpful discussions, Lianhe Shu and Ping Wang for assistance in scale up, and Anjula Pamidimukkala for providing PK data.

■ ABBREVIATIONS USED

APC, allophycocyanin; BMD, bone mineral density; DIO, diet induced obese; EE-RxR α , ligand binding domain of retinoid X receptor with EE tag; H6-TR- α , ligand binding domain of thyroid hormone receptor α with hexa His tag; H6-THR- β , ligand binding domain of thyroid hormone receptor β with hexa His tag; LXR, liver X receptor; α -MHC, α -myosin heavy chain; NAFLD, nonalcoholic fatty liver disease; NASH, nonalcoholic steatohepatitis; T3, triiodothyronine; T4, thyroxine; TDI, time dependent inhibition; TEMPO, 2,2,6,6-tetramethylpiperidin-1-yl)oxy; TG, triglyceride; TH, thyroid hormone; THR, thyroid hormone receptor; THR- α , thyroid hormone receptor α ; THR- β , thyroid hormone receptor β ; TSH, thyroid stimulating hormone

■ REFERENCES

- (1) Waters, D. D. Lipid treatment assessment project 2: a multinational survey to evaluate the proportion of patients achieving low-density lipoprotein cholesterol goals. *Circulation* **2009**, *120*, 28–34.
- (2) Joy, T. R.; Hegele, R. A. Narrative review: statin-related myopathy. *Ann. Intern. Med.* **2009**, *150*, 858–868.
- (3) DeFronzo, R. A.; Ferrannini, E. Insulin resistance. A multifaceted syndrome responsible for NIDDM, obesity, hypertension, dyslipidemia, and atherosclerotic cardiovascular disease. *Diabetes Care* **1991**, *14*, 173–194.
- (4) Cazanave, S. C.; Gores, G. J. Mechanisms and clinical implications of hepatocyte lipoapoptosis. *Clin. Lipidol.* **2010**, *5*, 71–85.

- (5) Grover, G. J.; Mellström, K.; Ye, L.; Malm, J.; Li, Y.-L.; Bladh, L.-G.; Sleph, P. G.; Smith, M. A.; George, R.; Vennström, B.; Mookhtiar, K.; Horvath, R.; Speelman, J.; Egan, D.; Bäter, J. D. Selective thyroid hormone receptor-beta activation: a strategy for reduction of weight, cholesterol, and lipoprotein (a) with reduced cardiovascular liability. *Proc. Natl. Acad. Sci. U.S.A.* **2003**, *100*, 10067–10072.

- (6) Grover, G. J.; Egan, D. M.; Sleph, P. G.; Seehler, B. C.; Chiellini, G.; Nguyen, N.-H.; Baxter, J. D.; Scanlan, T. S. Effects of the thyroid hormone receptor agonist GC-1 on metabolic rate and cholesterol in rats and primates: selective actions relative to 3,5,3'-triiodo-L-thyronine. *Endocrinology* **2004**, *145*, 1656–1661.

- (7) Johansson, L.; Rudling, M.; Scanlan, T. S.; Lundåsen, T.; Webb, P.; Baxter, J.; Angelin, B.; Parini, P. Selective thyroid receptor modulation by GC-1 reduces serum lipids and stimulates steps of reverse cholesterol transport in euthyroid mice. *Proc. Natl. Acad. Sci. U.S.A.* **2005**, *102*, 10297–10302.

- (8) Morkin, E.; Pennock, G. D.; Spooner, P. H.; Bahl, J. J.; Goldman, S. Clinical and experimental studies on the use of 3,5-diiodothyropropionic acid, a thyroid hormone analogue, in heart failure. *Thyroid* **2002**, *12*, 527–533.

- (9) Bassett, J. H.; Williams, G. R. The molecular actions of thyroid hormone in bone. *Trends Endocrinol. Metab.* **2003**, *14*, 356–364.

- (10) Simonides, W. S.; Thelen, M. H. M.; van der Linden, C. G.; Muller, A.; van Hardeveld, C. Mechanism of thyroid-hormone regulated expression of the SERCA genes in skeletal muscle: implications for thermogenesis. *Biosci. Rep.* **2001**, *21*, 139–154.

- (11) Klein, I.; Danzi, S. Thyroid disease and the heart. *Circulation* **2007**, *116*, 1725–1735.

- (12) Joharapurkar, A. A.; Dhote, V. V.; Jain, M. R. Selective thymimetics using receptor and tissue selectivity approaches: prospects for dyslipidemia. *J. Med. Chem.* **2012**, *55*, 5649–5675.

- (13) Dow, R. L.; Schneider, S. R.; Paight, E. S.; Hank, R. F.; Chiang, P.; Cornelius, P.; Lee, E.; Newsome, W. P.; Swick, A. G.; Spitzer, J.; Hargrove, D. M.; Patterson, T. A.; Pandit, J.; Chrunyk, B. A.; LeMotte, P. K.; Danley, D. E.; Rosner, M. H.; Ammirate, M. J.; Simons, S. P.; Schulte, G. K.; Tate, B. F.; DaSilve-Jardine, P. Discovery of a novel series of 6-azauracil-based thyroid hormone receptor ligands: potent, TR β subtype-selective thymimetics. *Bioorg. Med. Chem. Lett.* **2003**, *13*, 379–382.

- (14) Berkenstam, A.; Kristensen, J.; Mellström, K.; Carlsson, B.; Malm, J.; Rehnmark, S.; Garg, N.; Andersson, C. M.; Rudling, M.; Sjöberg, F.; Angelin, B.; Baxter, J. D. The thyroid hormone mimetic compound KB2115 lowers plasma LDL cholesterol and stimulates bile acid synthesis without cardiac effects in humans. *Proc. Natl. Acad. Sci. U.S.A.* **2008**, *105*, 663–667.

- (15) Ladenson, P. W.; Kristensen, J. D.; Ridgway, E. C.; Olsson, A. G.; Carlsson, B.; Klein, I.; Baxter, J. D.; Angelin, B. Use of the thyroid hormone analogue eprotirome in statin-treated dyslipidemia. *N. Engl. J. Med.* **2010**, *362*, 906–916.

- (16) Erion, M. D.; Cable, E. E.; Ito, B. R.; Jiang, H.; Fujitaki, J. M.; Finn, P. D.; Zhang, B.-H.; Hou, J.; Boyer, S. H.; van Poelje, P. D.; Linemeyer, D. L. Targeting thyroid hormone receptor- β agonists to the liver reduces cholesterol and triglycerides and improves the therapeutic index. *Proc. Natl. Acad. Sci. U.S.A.* **2007**, *104*, 15490–15495.

- (17) Garg, N.; Rao, V. M.; Gandhi, R. B.; Washburn, W. N.; Koehler, K.; Malm, J. Stable oral pharmaceutical composition containing thyroid hormone receptor agonists. US 20090220598, 2009.

- (18) Woltering, M.; Haning, H.; Schmidt, G.; Pernerstorfer, J.; Bischoff, H.; Kretschmer, A.; Vöhringer, V.; Faeste, C. Indazoles having an action similar to that of a thyroid hormone. Method for the production thereof and their use in medicaments. WO200222586, 2002.

- (19) Haning, H.; Schmidt, G.; Pernerstorfer, J.; Schneck, C.; Müller, U.; Bischoff, H.; Vöhringer, V.; Reinemer, P.; Apeler, H.; Schmidt, D.; Jonghaus, W.; Faeste, C.; Zoche, M.; Hauswald, M.; Woltering, M.; Kretschmer, A. Indoles for treating diseases that can be treated using thyroid hormones. WO200170687, 2001.

- (20) Taub, R.; Chiang, E.; Chabot-Blanchet, M.; Kelly, M. J.; Reeves, R. A.; Guertin, M.-C.; Tardif, J.-C. Lipid lowering in healthy volunteers treated with multiple doses of MGL-3196, a liver-targeted thyroid hormone receptor- β agonist. *Atherosclerosis* **2013**, *230*, 373–380.
- (21) Samaritoni, J. G. Homolytic alkylation of 3,6-dichloropyridazine. *Org. Prep. Proced. Int.* **1988**, *20* (1–2), 117–121.
- (22) Gardner, P. D.; Rafsanjani, H. S.; Rand, L. Reaction of phenolic Mannich base methiodides and oxides with various nucleophiles. *J. Am. Chem. Soc.* **1959**, *81*, 3364–3367.
- (23) Chen, Y. L.; Ruggeri, S. The process for converting 2,4-dichloropyridines into 2-aryloxy-4-chloropyridines. WO 199639388, 1996.
- (24) Hickey, D. M. B.; Leeson, P. D.; Novelli, R.; Shah, V. P.; Burpitt, B. E.; Crawford, L. P.; Davies, B. J.; Mitchell, M. B.; Pancholi, K. D.; Tuddenham, D.; Lewis, N. J.; O'Farrell, C. Synthesis of thyroid hormone analogues. Part 3. Iodonium salt approaches to SK&F L-94901. *J. Chem. Soc., Perkin Trans. 1* **1988**, 3103–3111.
- (25) Anelli, P. L.; Biffi, C.; Montanari, F.; Quici, S. Fast and selective oxidation of primary alcohols to aldehydes or to carboxylic acids and of secondary alcohols to ketones mediated by oxoammonium salts under two-phase conditions. *J. Org. Chem.* **1987**, *52*, 2559–2562.
- (26) Salturo, F.; Bemis, G.; Gao, H. Inhibitors of p38. WO 200017204, 2000.
- (27) Law, H.; Dukat, M.; Teitler, M.; Lee, D. K. H.; Mazzocco, L.; Kamboj, R.; Rampersad, V.; Prisinzano, T.; Glennon, R. A. Benzylimidazolines as h5-HT_{1B/1D} serotonin receptor ligands: a structure–affinity investigation. *J. Med. Chem.* **1998**, *41*, 2243–2251.
- (28) Sotelo, E.; Ravina, E. Pyridazine derivatives. XXIV. Efficient N-methylation of diversely substituted 3(2H)-pyridazinones using N,N-dimethylformamide dimethyl acetal. *Synth. Commun.* **2002**, *32* (11), 1675–1680.
- (29) Carroll, R. D.; Miller, M. W.; Mylari, B. L.; Chappel, L. R.; Howes, H. L., Jr.; Lynch, M. J.; Gupta, S. K.; Rash, J. J.; Koch, R. C. Anticoccidial derivatives of 6-azauracil. 5. Potentiation by benzophenone side chains. *J. Med. Chem.* **1983**, *26*, 96–100.
- (30) Yoshihara, H. A. L.; Apriletti, J. W.; Baxter, J. D.; Scanlan, T. S. Structural determinants of selective thymomimetics. *J. Med. Chem.* **2003**, *46*, 3152–3161.
- (31) Ye, L.; Li, Y.-L.; Mellström, K.; Mellin, C.; Bladh, L.-G.; Koehler, K.; Garg, N.; Collazo, A. M. G.; Litten, C.; Husman, B.; Persson, K.; Ljunggren, J.; Grover, G.; Sleph, P. G.; George, R.; Malm, J. Thyroid receptor ligands. I. Agonist ligands selective for the thyroid receptor β_1 . *J. Med. Chem.* **2003**, *46*, 1580–1588.
- (32) Boyer, S. H.; Jiang, H.; Jacintho, J. D.; Reddy, M. V.; Li, H.; Li, W.; Godwin, J. L.; Schulz, W. G.; Cable, E. E.; Hou, J.; Wu, R.; Fujitaki, J. M.; Hecker, S. J.; Erion, M. D. Synthesis and biological evaluation of a series of liver-selective phosphonic acid thyroid hormone receptor agonists and their prodrugs. *J. Med. Chem.* **2008**, *51*, 7075–7093.
- (33) Nascimento, A. S.; Dias, S. M. G.; Nunes, F. M.; Aparicio, R.; Ambrosio, A. L. B.; Bleicher, L.; Figueira, A. C. M.; Santos, M. A. M.; de Oliveira Neto, M.; Fischer, H.; Togashi, M.; Craievich, A. F.; Garratt, R. C.; Baxter, J. D.; Webb, P.; Polikarpov, I. Structural rearrangements in the thyroid hormone receptor hinge domain and their putative role in the receptor function. *J. Mol. Biol.* **2006**, *360*, 586–598.
- (34) (a) Reynolds, C. H. Computer-aided drug design: a practical guide to protein-structure based modeling. In *Drug Design: Ligand and Structure Based Approaches*; Merz, K. M., Ringe, D., Reynolds, C. H., Eds.; Cambridge University Press: Cambridge, U.K., 2010; pp 181–196. (b) Kangas, E.; Tidor, B. Optimizing electrostatic affinity in ligand–receptor binding: theory, computation, and ligand properties. *J. Chem. Phys.* **1998**, *109*, 7522–7545.
- (35) Danzi, S.; Klein, I. Cardiac specific effects of thyroid hormone analogues. *Horm. Metab. Res.* **2011**, *43*, 737–742.
- (36) Taub, R.; Grinsby, J.; Larigan, J. D.; Pietranico, S.; Dvorozniak, M.; Conde-Knape, K. Unpublished results.
- (37) *MacPymol*; DeLano Scientific LLC: South San Francisco, CA, 2006.
- (38) Halgren, T. A. Merck molecular force field. I. Basis, form, scope, parameterization, and performance of MMFF94. *J. Comput. Chem.* **1996**, *17*, 490–519.
- (39) *Molecular Operating Environment (MOE)*, version 2012.10; Chemical Computing Group Inc. (1010 Sherbooke St. West, Suite 910, Montreal, QC, Canada, H3A 2R7), 2012.